JOURNAL OF COMPUTATIONAL PHYSICS 17, 53–67 (1975)

Solving the Conservation Equations in Fuel Rod Bundles Exposed to Parallel Flow by Means of Curvilinear–Orthogonal Coordinates

R. MEYDER

Gesellschaft für Kernforschung m.b.H., 7500 Karlsruhe, Postfach 3640, Federal Republic of Germany

Received April 19, 1974; revised October 9, 1974

In this paper a method is described for constructing a curvilinear–orthogonal mesh grid. A method to perform calculations in such mesh grid is also illustrated. The method is demonstrated for the problem of laminar flow in rod bundle geometry. The comparison of the results with those of other authors is good.

1. INTRODUCTION

In designing nuclear reactors with smooth fuel rods the most precise information possible is wanted about the stresses acting upon the fuel rod claddings, i.e., on the temperatures and temperature gradients to which they are subjected, in order to allow an optimum selection of fuel rod pitch, diameter, and wall thickness as well as the tolerances to be imposed on these quantities. These data are especially important for fuel elements with high radial power gradient, for all corner and wall rods, and for the case of perturbations in the fuel rod arrangement. Since the effects of these perturbations and those of the fuel element box walls are not limited to the vicinity of a single fuel rod, an area including several fuel rods must be taken into consideration. The conservation equations must be solved in order to obtain the temperatures and temperature gradients in such an area. A problem of special difficulty here is the determination of the velocity and temperature fields in the coolant between the fuel rods. The coupled conservation equations for mass, impulse, and enthalpy must be solved in a complicated geometry.

Turbulent flow has been calculated successfully, allowing for molecular and eddy viscosities in channel and plate flows having a simple geometry with differential approximations for the conservation equations [1, 2, 3, 4]. If the eddy viscosity

is known as a function of the location, a conclusion about the turbulent exchange parameter for the heat can be derived, for instance, by using the Reynolds analogy or other suitable conversion schemes. This means that the heat transport problem for this flow can be solved too [2, 4]. One important prerequisite to a successful solution is that the flow cross section under consideration should be simple to describe in the coordinate system used.

A good description requires that the following prerequisites be met.

(1) The area boundary lines shall be the coordinate lines. Where a boundary line coincides with a coordinate line it is easy to state the boundary conditions precisely. And a precise statement of the boundary conditions is one prerequisite for a satisfactory solution.

(2) A selective microsubdivision must be possible in areas subject to major function value changes. As a rule, the accuracy of the approximation of the function will decrease with increasing difference between two neighboring function values, so that it is desirable to be able to select a smaller subdivision in such areas.

(3) A satisfactory result must be obtained from a minimum number of points. This means that a minimum of storage capacity and short computation times are required for one computation run, so that a major part of a fuel element can be treated in one computation run.

(4) The grid points must be arranged in accordance with simple laws, i.e., the same number of mesh points must be encountered in each line or column of the matrix. In that case, geometrically adjacent points in the data field can always be arranged on the computer in accordance with the sketch shown below. When this requirement is met, processing the field, i.e., establishing and solving the system of differential equations, will be facilitated considerably, for, if we have established the equation for a point (i, j), it will suffice to vary the indices i and j in order to describe the entire region (see Fig. 1).

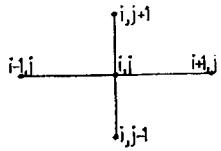

FIG. 1. Simple-law mesh grid.

All of these four requirements are met by the curvilinear–orthogonal coordinate system shown in Fig. 2 for the geometry of a rod bundle, while all the other conventional coordinate systems meet only one, or at best two, of these prerequisites.

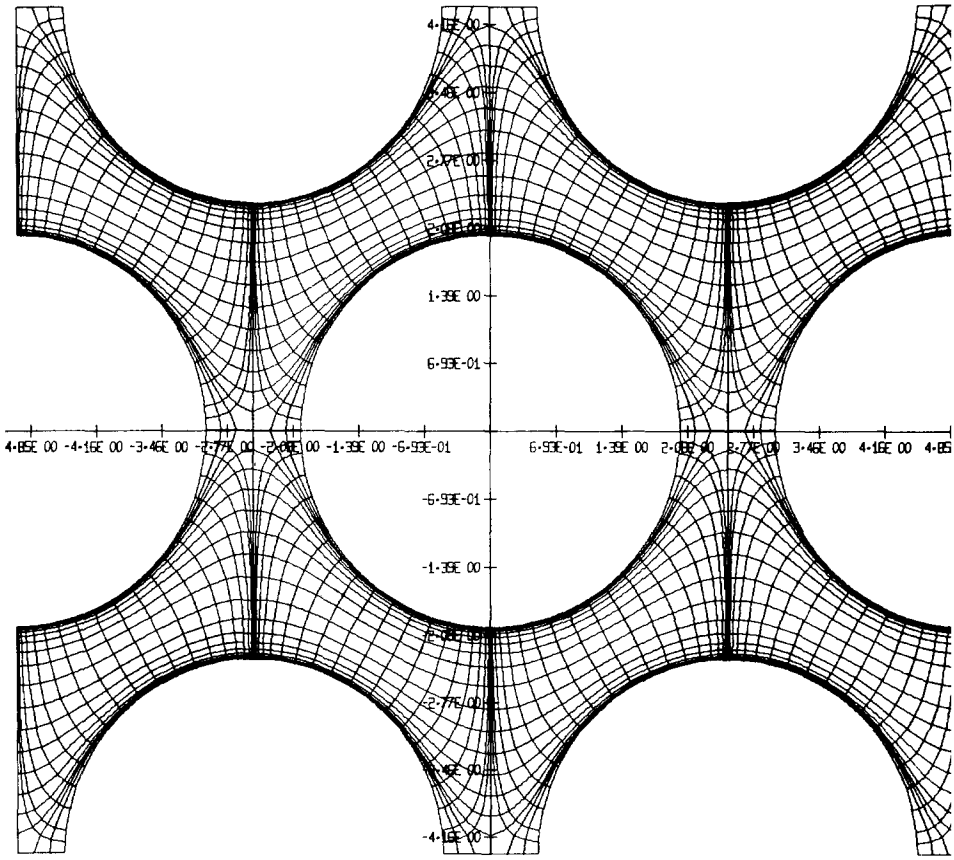

FIG. 2. Representation of a fuel-element section having a hexagonal fuel rod arrangement, using a curvilinear–orthogonal grid of 40 × 80 points. The grid points have been connected linearly.

1a. NOTATIONS

Symbol	Unit	Designation
D	m	fuel rod diameter
D_h	m	hydraulic diameter
F^{ij}	N	force
P	m	fuel rod pitch
p	N/m^2	pressure
$S1$, $S2$, $S3$	m	coordinate line
v^1	m/sec	velocity in the $S1$- or z-direction
$\bar{v}$	m/sec	mean velocity, referred to channel cross-section area
μ	kg/msec	dynamic viscosity
$x1$, $x2$, $x3$	m	Cartesian coordinates

2. COMPUTATION WITH CURVILINEAR–ORTHOGONAL COORDINATES USING THE EXAMPLE OF THE NAVIER–STOKES EQUATION

The theory of the treatment of problems in general curvilinear–orthogonal coordinate systems is not new [6], yet it is hardly ever used for computations. Thus the author is aware of the treatment of only one stability problem in curvilinear–orthogonal coordinates [7]. However, in [7] there was only qualitative agreement of the results with the results obtained via other procedures (such as the finite-elements method). Unlike the tensor presentation used in [7], the problem equation here is derived from a curvilinear–orthogonal volume element of known dimensions. It was found empirically that improved accuracy is obtained if the arc length itself rather than differential geometry representations of the arc length (i.e., involving the metric components) is used in the finite-difference equation. In geometries where one or more metric components are strongly varying, the differential geometry expressions for arc length are poorly approximated, which probably explains why only qualitative agreement was found in [7].

The Navier–Stokes equation for three-dimensional flow consists of three coupled differential equations. However, we shall stipulate that it is sufficient for the description of our flow problem to consider only one velocity direction, that the fluid properties are constant, and that we are concerned with a steady-state,

laminar, fully developed flow in a channel of noncircular cross section. In that case, we obtain only the following equation, using Cartesian coordinates.

$$\partial p/\partial x1 = \mu((\partial^2 v^1/\partial x2^2) + (\partial^2 v^1/\partial x3^2)). \tag{1}$$

This is a balance of forces in the z-direction on a volume element. We shall now derive the corresponding difference equation, using a volume element of the type shown in Fig. 3.

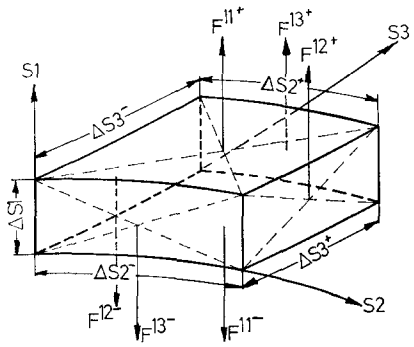

FIG. 3. Curvilinear-orthogonal volume element.

Since we shall consider a duct flow, as stipulated in Fig. 3, $S1$ is selected as a straight line. Coordinate lines $S2$ and $S3$ shall be curvilinear-orthogonal coordinates in the plane perpendicular to $S1$.

Since there is a velocity only in the $S1$-direction, the forces will be:

$$F^{11+} = -p^+ \cdot ((\Delta S2^+ + \Delta S2^-)/2) \cdot ((\Delta S3^+ + \Delta S3^-)/2), \tag{2}$$

$$F^{11-} = +p^- \cdot ((\Delta S2^+ + \Delta S2^-)/2) \cdot ((\Delta S3^+ + \Delta S3^-)/2), \tag{3}$$

$$F^{12+} = (\mu(\Delta v^1/\Delta S2))^+ \cdot \Delta S1 \cdot \Delta S3^+, \tag{4}$$

$$F^{12-} = -(\mu(\Delta v^1/\Delta S2))^- \cdot \Delta S1 \cdot \Delta S3^-, \tag{5}$$

$$F^{13+} = (\mu(\Delta v^1/\Delta S3))^+ \cdot \Delta S1 \cdot \Delta S2^+, \tag{6}$$

$$F^{13-} = -(\mu(\Delta v^1/\Delta S3))^- \cdot \Delta S1 \cdot \Delta S2^-. \tag{7}$$

With respect to the problem under consideration these are all the forces affecting the volume element; hence

$$0 = F^{11+} + F^{11-} + F^{12+} + F^{12-} + F^{13+} + F^{13-}, \tag{8}$$

or, expressed by the right-hand sides of (2)–(7),

$$0 = -(p^+ - p^-) \cdot \left(\frac{\Delta S2^+ + \Delta S2^-}{2}\right) \cdot \left(\frac{\Delta S3^+ + \Delta S3^-}{2}\right)$$
$$+ \mu \cdot \Delta S1 \left(\frac{\Delta v^{1^+}}{\Delta S2} \cdot \Delta S3^+ - \frac{\Delta v^{1^-}}{\Delta S2} \cdot \Delta S3^- + \frac{\Delta v^{1^+}}{\Delta S3} \cdot \Delta S2^+ - \frac{\Delta v^{1^-}}{\Delta S3} \cdot \Delta S2^-\right). \quad (9)$$

Dividing, as usual, the equation by the volume of the element, we obtain the difference equation

$$0 = -\frac{p^+ - p^-}{\Delta S1} + \frac{4\mu}{(\Delta S2^+ + \Delta S2^-) \cdot (\Delta S3^+ + \Delta S3^-)}$$
$$\cdot \left(\frac{\Delta v^{1^+}}{\Delta S2} \cdot \Delta S3^+ - \frac{\Delta v^{1^-}}{\Delta S2} \cdot \Delta S3^- + \frac{\Delta v^{1^+}}{\Delta S3} \cdot \Delta S2^+ - \frac{\Delta v^{1^-}}{\Delta S3} \cdot \Delta S2^-\right). \quad (10)$$

This equation is easily transformed into a well-known form depending on the definition of the coordinate lines.

For instance, if we state that

$$S1 = z \qquad \text{so that} \quad \Delta S1 = \Delta z, \quad (11)$$

$$S2 = r \qquad \text{so that} \quad \Delta S2^+ = \Delta S2^- = \Delta S2 = \Delta r, \quad (12)$$

and

$$S3 = r \cdot \phi \qquad \text{so that} \quad \Delta S3^+ = (r + (\Delta r/2)) \cdot \Delta\phi;$$
$$\Delta S3^- = (r - (\Delta r/2)) \cdot \Delta\phi;$$
$$\Delta S3 = r \cdot \Delta\phi, \quad (13)$$

after some rearrangement we find

$$0 = -\frac{\Delta p}{\Delta z} + \mu$$
$$\times \left(\frac{\left(\frac{\Delta v^1}{\Delta r}\right)^+ - \left(\frac{\Delta v^1}{\Delta r}\right)^-}{\Delta r} + \frac{\left(\frac{\Delta v^1}{\Delta r}\right)^+ + \left(\frac{\Delta v^1}{\Delta r}\right)^-}{2r} + \frac{\left(\frac{\Delta v^1}{r \cdot \Delta\phi}\right)^+ - \left(\frac{\Delta v^1}{r \cdot \Delta\phi}\right)^-}{r \cdot \Delta\phi}\right). \quad (14)$$

If $0.5 \cdot ((\Delta v^1/\Delta r)^+ + (\Delta v^1/\Delta r)^-) = \Delta v^1/\Delta r$, then passing to the limits yields to

$$0 = -\frac{\partial p}{\partial z} + \mu \left(\frac{\partial^2 v^1}{\partial r^2} + \frac{1}{r} \cdot \frac{\partial v^1}{\partial r} + \frac{1}{r^2} \cdot \frac{\partial^2 v^1}{\partial \phi^2}\right). \quad (15)$$

Consequently, in order to establish difference equations we must know only the local dimensions of one mesh unit, i.e., lengths and areas and/or angles. However, these lengths and angles can vary from one mesh unit to the next. This is the basic difference compared to a Cartesian coordinate system. While, as a rule, the dimen-

sions of all mesh units in a Cartesian system are equal, the dimensions differ in curvilinear systems.

Where curvilinear coordinate lines are given as functions, as in a Cartesian coordinate system, the lengths and angles of the curvilinear coordinate system can be determined with the aid of differential geometry [6]. This will yield the information on local lengths and angles in a form suitable for direct use in the tensor calculus usually employed for curvilinear systems, i.e., in the metric tensor and in the Christoffel symbols. Although in the method described here, as we shall explain in Section 3, the coordinate lines are available only as point data; the metric tensors and Christoffel symbols can be determined readily, since these can be calculated from the basis vectors which are determined by the arc length and the potential difference between two neighboring points (see Section 3). This

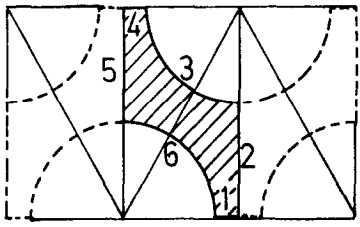

FIG. 4. Schematic representation of the selected fuel rod bundle section.

will ensure that later these coordinate systems can also be used to calculate flows having three velocity directions with the aid of tensor calculus.

Like the Navier–Stokes equation it is possible, of course, to treat the energy equation in curvilinear–orthogonal coordinates.

Hence, these coordinates are a suitable means for representing the conservation equations in a fuel rod bundle geometry, under the four requirements defined in Section 1.

3. GENERATION OF A CURVILINEAR–ORTHOGONAL COORDINATE SYSTEM

In order to facilitate the discussion, the individual sections of the boundary curve are numbered consecutively (Fig. 4). This boundary curve has six corners. However, the desired mesh grid should have only four corners, which means that two angles must be "straightened out." It is seen from Fig. 2 that the corners (1, 2) and (4, 5) have been straightened out.

Hence, we can state that corners (6, 1), (2, 3), (3, 4), (5, 6) will remain corners even in the curvilinear grid network.

Now, how can we find orthogonal coordinate lines in the given area? We know

that orthogonal lines occur in potential theory. For instance, in an electric field there will be field lines between the two plates of a capacitor, i.e., equipotential lines and lines of force, i.e., the gradient lines of the potential field. Both types of lines are perpendicular to each other throughout the field, and in particular, at the field edges. Both types of lines satisfy the potential equation. Hence, we must merely solve the potential equation twice in the area of interest, first stating the boundary conditions for the potential, and, second, for the force lines. The boundary conditions for the potential were selected as follows:

Section 4, 5	charge $\phi = 100$,
Section 1, 2	charge $\phi = 0$,
Section 3	$\partial\phi/\partial n = 0$,
Section 6	$\partial\phi/\partial n = 0$.

The boundary conditions for the force lines:

Section 3	force $\psi = 0$,
Section 6	force $\psi = 100$,
Section 4, 5	$\partial\psi/\partial n = 0$,
Section 1, 2	$\partial\psi/\partial n = 0$.

Using the grid shown in Fig. 5 and the successive-point-overrelaxation method, the potential equations are solved. When a solution has been established, the potential values of the equipotential lines are determined by division in the desired manner of the boundary curve with $\partial\phi/\partial n = 0$ and by determination of the

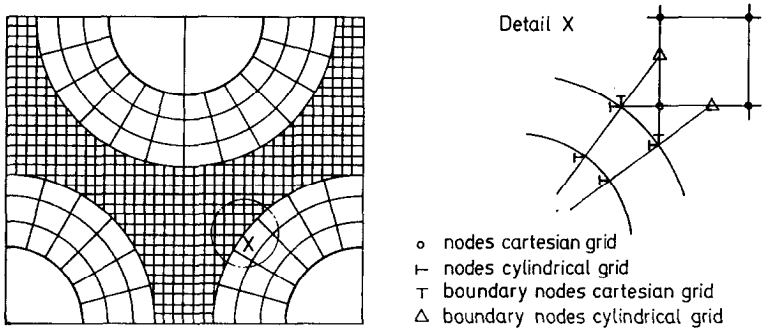

FIG. 5. Description of a fuel rod bundle by means of mixed cylindrical–Cartesian coordinates. The function value for the boundary nodes of the cylindrical grid are interpolated between the adjacent nodes of the Cartesian grid.

appropriate potential values. The solution field is then scanned for neighboring mesh points for which the value of a searched equipotential line lies between their potential values. If such a situation is detected, one point of the equipotential line is calculated by a local third-order interpolation polynomial for the potential field along the appropriate mesh line. When the field and force lines are known (as point data), the point of intersection of these lines must be determined. Therefore, first those points of the field and force lines are searched with the point of intersection lying in between. Then local third-order polynomials are set up for both lines, and their point of intersection is calculated. The equipotential line between two intersection points now yields the initial point, some intermediate points, and the final point. The arc length between the points of intersection is then determined by summing up the linear distances between these points.

Thus the geometry data required to solve Eq. (10) have been determined.

A somewhat different method of determining a curvilinear–orthogonal coordinate system for a given region is described by Barfield [8]. In this method, the boundary curve of the area of interest is first mapped on a circle and then the latter on a rectangle. The Cartesian image area obtained is used to compute the coordinates of the grid points, in a manner similar to the technique described in this section. The advantage of this method is that, due to the conformal mapping, regions having a great variety of boundary curves can be considered, whereas in the method described in this paper, any change in the type of the boundary curve will require changes in the computer program. The difference between the method presented here and that of [8] is: If (X, Y) are the curvilinear coordinates and (x, y) are the rectangular Cartesian coordinates, the method of [8] finds the mapping functions $x(X, Y)$, $y(X, Y)$, whereas the present method finds the inverse mapping.

4. Results for Laminar Velocity Fields and Discussion

The determination of the orthogonal mesh grid, i.e., the computation of the position of the grid points, the distances between grid points, and solving of Eq. (10), is accomplished by means of the *KROKOPI PL*/1 computer code (*KR*ummling-*O*rthogonale *KO*ordinaten in *PI*ngeometrie). This program requires about 100 *k* program storage and about 250 to 350 *k* data storage, depending on the parameters selected. Computation times on the IBM 370/165 are about 5 to 7 min. The curvilinear–orthogonal coordinate system is generated by solving the potential equations cited in Section 3.

Incorporated into this program is the solution of Eq. (10) in curvilinear–orthogonal coordinates. The user of this program, therefore, acquires not only geometry data, but at the same time a statement as to the reliability of these data in describing the geometry (Figs. 11, 12).

Figures 6–9 show some plots of the results. On the left-hand sides of these figures the grid systems are shown which were used to compute the flow in question, and on the right-hand sides are the lines of equal velocity within this flow. The velocity differences between the lines decrease by the square, starting out from the wall.

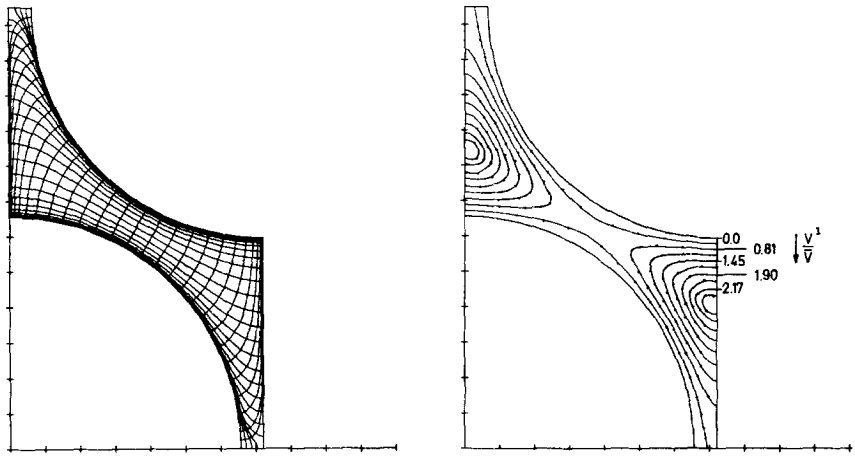

FIG. 6. Isotachs of laminar flow in a hexagonal fuel rod bundle $P/D = 1.1$. This flow was determined by means of the coordinate system shown on the left.

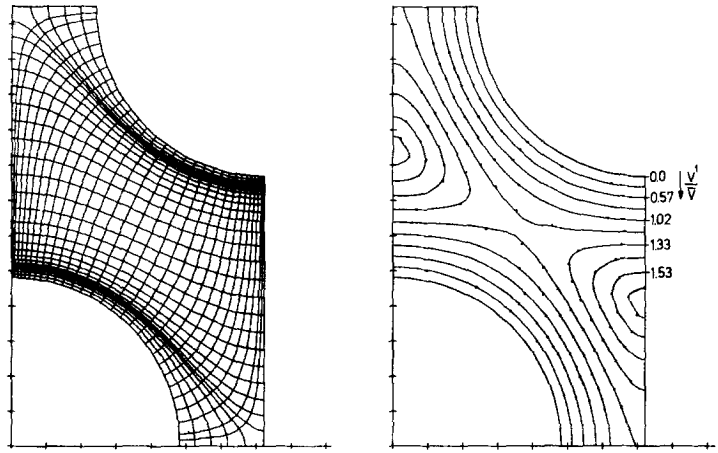

FIG. 7. Isotachs of laminar flow in a hexagonal fuel rod bundle $P/D = 1.5$. This flow was determined by means of the coordinate system shown on the left.

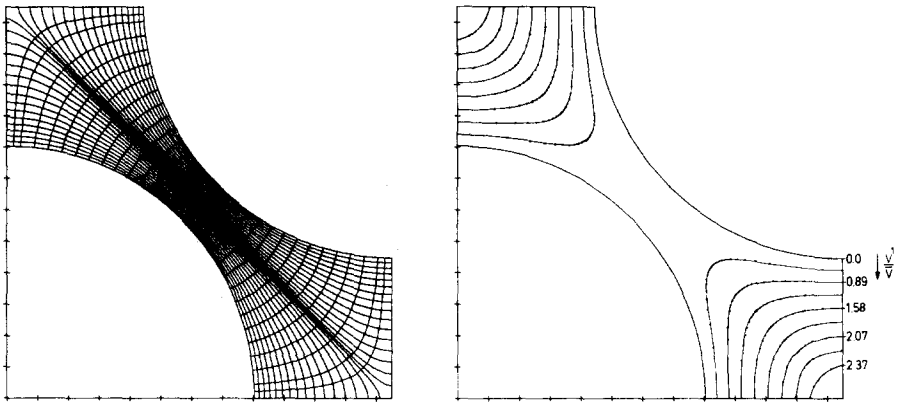

FIG. 8. Isotachs of laminar flow in a square fuel rod bundle $P/D = 1.1$. This flow was determined by means of the coordinate system shown on the left.

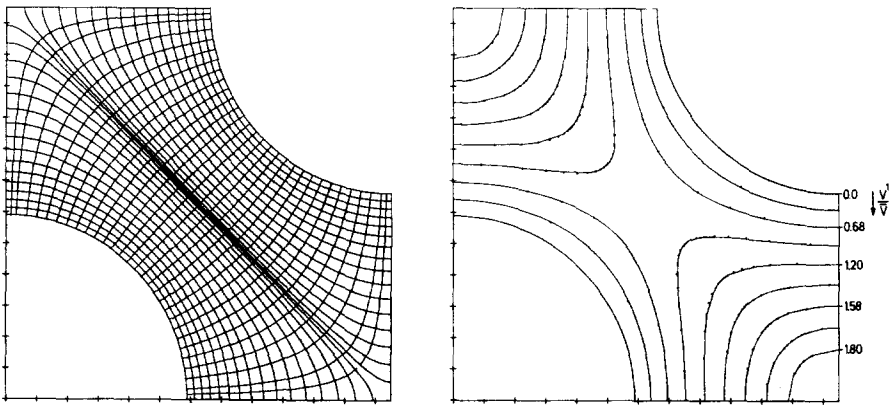

FIG. 9. Isotachs of laminar flow in a square fuel rod bundle $P/D = 1.5$. This flow was determined by means of the coordinate system shown on the left.

These figures clearly reflect the flexibility and capabilities of the coordinate system used, especially if we consider that all the coordinate systems include only 31×31 points.

Two different criteria must be taken into consideration for an evaluation of results. For one, the solution must be consistent in itself, meaning that, for instance, where the same function value is obtained at different locations for reasons of symmetry, the values achieved in the solution must be the same, within acceptable tolerance limits. For another, the results obtained via this procedure for a laminar flow can be compared to the results obtained by other authors [5].

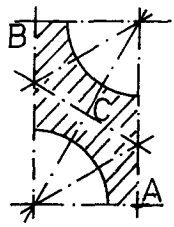

FIG. 10. Plot of the symmetry lines of a hexagonal fuel rod arrangement.

In the case of symmetry validation where a hexagonal fuel rod arrangement is used, the function value at point A or B (cf. Fig. 10) can be compared to that at point C. This was verified for different fuel rod pitch-to-diameter ratios (P/D ratios), and the results are plotted in Fig. 11.

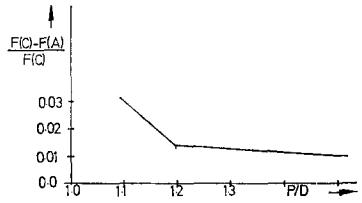

FIG. 11. Maximum symmetry error as a function of the P/D ratio, hexagonal rod arrangement.

As expected, the error will rise with decreasing P/D ratio; however, it remains within tolerable limits.

While a comparison of the function values in A and C (cf. Fig. 10) yields a statement on the representation of the geometry for the hexagonal fuel rod arrangement, this does not apply to a square fuel rod arrangement. Therefore, the equation describing the coordinate system for this type of arrangement (potential equation) has been solved twice, using first a mixed cylindrical–Cartesian coordinate network to generate the curvilinear–orthogonal coordinates, and then the newly acquired curvilinear coordinate system (identity mapping).

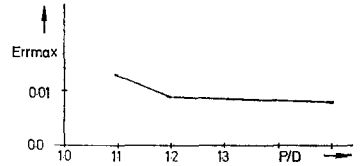

FIG. 12. Maximum errors caused by plotting in curvilinear–orthogonal coordinates, shown as a function of the P/D ratio, square fuel rod arrangement.

TABLE I

Ratio of Maximum Velocity to $\bar{v}$

	P/D	Present data	Rehme [5]
Hexagonal rod arrangement	1.1	2.28	2.43
	1.2	1.98	2.02
	1.3	1.78	1.79
	1.5	1.59	1.59
Square rod arrangement	1.1	2.47	2.46
	1.2	2.31	2.31
	1.5	1.88	1.89

TABLE II

Ratio of Saddle Point Velocity (Point C, Fig. 10) to $\bar{v}$

	P/D	Present data	Rehme [5]
Hexagonal rod arrangement	1.1	0.53	0.57
	1.2	0.90	0.91
	1.3	1.08	1.09
	1.5	1.22	1.22
Square rod arrangement	1.1	0.14	0.14
	1.2	0.38	0.38
	1.5	0.85	0.85

TABLE III

Geometry coeff. $K = 2 \cdot \Delta p \cdot D_h/\Delta z \cdot \bar{v}$

	P/D	Present data	Rehme [5]
Hexagonal rod arrangement	1.1	83.7	83.2
	1.2	100	101
	1.3	110	110
	1.5	125	122
Square rod arrangement	1.1	58.6	59
	1.2	81.0	81
	1.5	119	120

If the presentation were exact, the same potential value would be recovered at each grid point in the second solution as was found in the first computation. The maximum relative deviation between the first and second computations of the potential values has been plotted as a function of the P/D ratio in Fig. 12.

The maximum errors are encountered only in the corners, A and B (cf. Fig. 10).

Throughout the remaining field the errors are significantly lower (by one to two powers of 10).

Hence we can state that problem equations solved with the aid of these geometry data will have a maximum geometry related error of approximately 1–2 %. However, this error can still be reduced by using a smaller grid subdivision.

The results acquired in this paper shall now be compared to those obtained by Rehme [5]. Rehme represented a characteristic subchannel section by cylindrical coordinates and solved the equation numerically for a laminar flow.

Comparison with the results shown by Rehme in Tables I–III indicates very good agreement, especially since Rehme also stated an error of approximately 1 % for his values. The only remaining consideration is a comparison of the effort involved in the two solution procedures. If we do not include the effort required to determine the geometry data for the curvilinear–orthogonal coordinates, we will obtain Table IV.

TABLE IV

Comparison of the Effort Required to Plot This Characteristic Subchannel Section

	Cylindrical coordinates	Curvilinear–orthogonal coordinates
Points/area	approx 4,000	70 to 150
Computation time	approx 1 min	0.3 min
Transition to plotting a larger area	transition equation always required	transition equation required only where the P/D ratio changes

With respect to the computation time required for the curvilinear coordinates it should be noted that the program is not yet optimized in this respect.

These results have shown that initial expectations with respect to the economical representation of a fuel rod geometry by means of this procedure have been fully confirmed.

5. References

1. A. Quarmby, Improved application of the von Kármán similarity hypothesis to turbulent flows in ducts, *J. Mech. Engineering Sci.* **11** (1969), 14.
2. T. Cebeci, A. Smith, and G. Mosinskis, Solution of the incompressible turbulent boundary-layer equations with heat transfer, *J. Heat Transfer* **92** (1970), 133.

3. M. DOSHI AND W. GILL, An improved mixing length theory of turbulent heat and mass transfer, *Intern. J. Heat Mass Transfer* **14** (1971), 1355.
4. S. PATANKAR AND D. SPALDING, "Heat Transfer in Boundary Layers," 2nd ed., Intertext Books, London, 1970.
5. K. REHME, Laminarströmung in Stabbündeln, *Chem. Ing. Tech.* **43** (1971), 962.
6. DUSCHEK-HOCHRAINER, "Grundzüge der Tensorrechnung in analytischer Darstellung," Vols. 1–3, Springer, Vienna, 1960.
7. H. ROTHERT, Anwendung der Schalentheorie auf hyperbolische Parabolide, Jahresverzeichnis der Hochschulschriften der DDR, der BRD und West-Berlin (VEB-Verlag). Ph.D. Thesis: Ruhr-Universität Bochum, 1970.
8. W. BARFIELD, Numerical method for generating orthogonal Curvilinear Meshes, *J. Computational Phys.* **5** (1970), 23.